

CHEMISTRY OF MATERIALS

VOLUME 17, NUMBER 4

FEBRUARY 22, 2005

© Copyright 2005 by the American Chemical Society

Articles

Nanoparticulate Palladium Supported by Covalently Modified Silicas: Synthesis, Characterization, and Application as Catalysts for the Suzuki Coupling of Aryl Halides

Robin B. Bedford,^{*,†} Udayshanker G. Singh,[‡] Richard I. Walton,^{*,†}
Ruth T. Williams,^{*,‡} and Sean A. Davis[§]

Department of Chemistry, University of Exeter, Stocker Road, Exeter, EX4 4QD, UK, Department of Chemistry, The Open University, Walton Hall, Milton Keynes, MK7 6AA, UK, and School of Chemistry, University of Bristol, Cantocks Close, Bristol BS8 1TS, UK

Received July 13, 2004. Revised Manuscript Received October 21, 2004

We present a study of the use of amine-functionalized, mesoporous silicas as supports for nanoparticulate palladium, and the use of the composite materials as heterogeneous catalysts for the Suzuki coupling of aryl bromides. Upon modification of the silica, via attachment of N-functionalized aminopropylsilyl ethers to surface silanol groups, only a small reduction in surface area and average pore diameter is observed. The mesoporosity and high surface area are also maintained after introduction of nanoparticulate palladium, as evidenced by the measurement of BET nitrogen sorption isotherms. Electron microscopy shows that the palladium particles are well-dispersed and of typical diameter 3–6 nm. Catalysis was initially tested using the coupling of phenylboronic acid with 4-bromoanisole in the presence of K_2CO_3 and with toluene as solvent. This revealed that the choice of organic modification has a crucial role in determining the activity and recyclability of the catalyst: optimum behavior was found for diamine- and triamine-containing systems, while quaternary alkylammonium salts showed poor activities. The optimized catalysts are also active in the coupling of a range of aryl bromides and phenylboronic acids, and after three catalytic runs they show virtually no drop in activity. Upon further cycling, however, and after six catalytic runs, we do observe a drop in activity, and this is accompanied by some leaching of palladium and pore-blocking by reaction products and byproducts.

Introduction

The use of transition-metal nanoparticles in the catalysis of organic transformations provides a powerful means for

the development of recyclable catalysts. There are a variety of methods for production of nanoparticles of transition metals and also a wide choice of solid supports ranging from polymers to ordered mesoporous silicas and microporous zeolites. Combining the metal nanoparticles with a support of choice gives a huge scope for the discovery of new, highly active catalysts for industrially important organic transforma-

* Corresponding authors. E-mail: r.bedford@ex.ac.uk (R.B.B.), r.i.walton@ex.ac.uk (R.I.W.), r.t.williams@open.ac.uk (R.T.W.).

[†] University of Exeter.

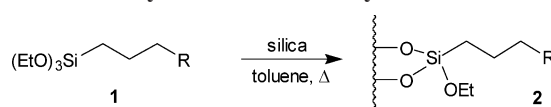
[‡] The Open University.

[§] University of Bristol.

tions, which may offer the additional advantage of being recyclable. The supported nanoparticle systems reported in the recent literature illustrate the variety of approaches to the materials: for example, gold particles can be introduced into mesoporous silica by direct interaction between colloidal gold and the solid silica,¹ by in situ reduction of chloroaurate in the presence of mesoporous silicas,² or by chemical modification of the silica surface with thiol moieties, followed by size-selective incorporation of gold particles.³ Bronstein et al. have recently stated that there are at least six distinctly different approaches to the incorporation of nanoparticles of metals into the pores of mesoporous hosts.⁴

Carbon–carbon bond-forming reactions have great utility in organic synthesis, and recent attention has been turned to the production of heterogeneous catalysts for this class of reactions, that may be easily separated from chemical reagents, and then reused.⁵ Transition-metal nanoparticles have found some considerable recent use as catalysts in carbon–carbon bond-forming reactions,⁶ and, although they are often used in the form of colloidal suspensions, there exists considerable scope for producing heterogeneous catalysts by supporting the nanoparticulate metal on high surface area, solid supports. Palladium and platinum are often the metals of choice in this class of reaction, and a number of recent publications have dealt with the immobilization of nanoparticles of these metals onto silica and alumina surfaces.^{7–18} The composite materials have been prepared using a variety of chemical approaches; for example, Wu et al. incorporated palladium in mesoporous silica during the synthesis of the silica itself,⁹ Okitsu et al. used a sonochemical approach to deposit Pd particles onto alumina from PdCl₂,¹⁰ Zhou et al. used a novel homogeneous approach via cyclodextrins and an ordered polystyrene bead array to

Scheme 1. Synthesis of Covalently Modified Silicas



give silicas with bimodal pore distributions, with Pd incorporated into the pore walls,¹² and Choudary et al. reduced PdCl₄²⁻ using hydrazine hydrate onto layered double hydroxide (LDH) supports.¹¹ In some cases, the materials produced by these routes have been assessed for their catalytic activity: Choudary et al. used their LDH materials as catalysts in the Heck reaction and found higher activities and selectivities than in homogeneous PdCl₂ systems,¹¹ Clark et al. also studied the Heck reaction with mesoporous silica-supported palladium and found a high degree of recyclability with respect to both activity and selectivity,⁸ and Mas-Marza et al. produced recyclable clay-supported Pd catalysts for the Sonogashira coupling reaction.¹⁵

The coupling of arylboronic acids with aryl halides, the Suzuki reaction, is perhaps the most powerful and versatile method for the formation of new biaryls.¹⁹ This is due to the ease of synthesis and handling coupled with the wide functional group tolerance of aryl boronic acids as compared to, for instance, Grignard reagents and also due to their relatively low toxicity (as compared to aryl tin reagents). Some recent publications have already focused upon developing new catalysts for the Suzuki reaction based on supported nanoparticulate palladium,^{20–23} but given the importance of the reaction, there is the need to investigate further suitable materials and to address the question of recyclability. In this paper, we assess a variety of novel silica-supported palladium nanoparticle materials as catalysts for the Suzuki coupling reaction. Our approach is to use chemical modification of the silicas with organic functionalities that may easily be tuned by choice of various alkyl chain lengths and functionalities. By surveying a variety of organic modifiers, we have optimized catalytic activity and developed highly active catalysts whose recyclability we then test.

Experimental Section

Materials. We chose to use a commercially available amorphous silica as our solid support, because our aim was to concentrate upon a survey of a range of organic modifications, rather than the synthesis of the silica itself. The silica used was Kieselgel 100, supplied by Aldrich. All other chemicals were supplied by either Aldrich or Lancaster and used as received. Solvents were distilled prior to use and stored over the appropriate drying agents. All reactions were performed under dry nitrogen conditions unless otherwise stated.

General Method for the Covalent Modification of Kieselgel 100. Scheme 1 shows the general method we have used for organic functionalization. Here, the structure of the product **2** is shown generalized as having two Si–O bonds to the surface; however,

- (1) Kónya, Z.; Puentes, V. F.; Kiricsi, I.; Zhu, J.; Ager, J. W.; Moon, K. K.; Frei, H.; Alivisatos, P.; Somorjai, G. A. *Chem. Mater.* **2003**, *15*, 1242.
- (2) Mukherjee, P.; Patra, C. R.; Ghosh, A.; Kumar, R.; Sastry, M. *Chem. Mater.* **2002**, *14*, 1678.
- (3) Mukherjee, P.; Sastry, M.; Kumar, R. *PhysChemComm* **2000**, 1–14, 4.
- (4) Bronstien, L.; Chernyshov, D. M.; Karlinsey, R.; Zwanziger, J. W.; Matveeva, V. G.; Sulman, E. M.; Demidenko, G. N.; Hentze, H.-P.; Antonietti, M. *Chem. Mater.* **2003**, *15*, 2623.
- (5) Bhanage, B. H.; Arai, M. *Catal. Rev.* **2001**, *43*, 315.
- (6) Moreno-Manos, M.; Pleixats, R. *Acc. Chem. Res.* **2003**, *36*, 638.
- (7) Bronstein, L.; Krämer, E.; Berton, B.; Burger, C.; Förster, S.; Antonietti, M. *Chem. Mater.* **1999**, *11*, 1402.
- (8) Clark, J. H.; Macquarrie, D. J.; Mubofu, E. B. *Green Chem.* **2000**, *2*, 53.
- (9) Wu, Y.; Zhang, L.; Li, G.; Liang, C.; Huang, X.; Zhang, Y.; Song, G.; Jia, J.; Zhixiang, C. *Mater. Res. Bull.* **2001**, *36*, 253.
- (10) Okitsu, K.; Yue, A.; Tanabe, S.; Matsumoto, H. *Chem. Mater.* **2000**, *12*, 3006.
- (11) Choudary, B. M.; Madhi, S.; Chowdari, N. S.; Kantam, M. L.; Sreedhar, B. *J. Am. Chem. Soc.* **2002**, *124*, 14127.
- (12) Zhou, Y.; Yu, S.-H.; Thomas, A.; Han, B.-H. *Chem. Commun.* **2003**, 262.
- (13) Fukuoka, A.; Araki, H.; Yuzuru, S.; Inanaki, S.; Fukushima, Y.; Ichikawa, M. *Inorg. Chim. Acta* **2003**, *350*, 371.
- (14) Yuranov, I.; Moeckli, P.; Suvorova, E.; Buffat, P.; Kiwi-Minsker, L.; Renken, A. *J. Mol. Catal. A: Chem.* **2003**, *192*, 239.
- (15) Mas-Mazra, E.; Segarra, A. M.; Claver, C.; Peris, E.; Fernandez, E. *Tetrahedron Lett.* **2003**, *44*, 6595.
- (16) Srivastava, R.; Venkathri, N.; Srinivas, D.; Ratnasamy, P. *Tetrahedron Lett.* **2003**, *44*, 3649.
- (17) Schwieger, W.; Gravenhorst, O.; Selvam, T.; Roessner, F.; Schlögl, R.; Su, D.; Mabande, G. T. P. *Colloid Polym. Sci.* **2003**, *281*, 584.
- (18) Canton, P.; Menegazzo, F.; Polizzi, S.; Pinna, F.; Pernicone, N.; Riello, P.; Fagherazzi, G. *Catal. Lett.* **2003**, *88*, 141.

- (19) For recent reviews, see: (a) Miyaura, N.; Suzuki, A. *Chem. Rev.* **1995**, *95*, 2457. (b) Stanforth, S. P. *Tetrahedron* **1998**, *54*, 263. (c) Suzuki, A. *J. Organomet. Chem.* **1999**, *576*, 147.
- (20) Kim, S. W.; Kim, M.; Lee, W. Y.; Hyeon, T. *J. Am. Chem. Soc.* **2002**, *124*, 7642.
- (21) Narayanan, R.; El-Sayed, M. A. *J. Am. Chem. Soc.* **2003**, *125*, 8340.
- (22) Biffis, A.; Sperotto, E. *Langmuir* **2003**, *19*, 9548.
- (23) Liu, Y. B.; Khemtong, C.; Hu, J. *Chem. Commun.* **2004**, 398.

the precise value may vary depending on the local surface coverage of silanol groups.

To degassed Kieselgel 100 (2.00 g) were added toluene (60 mL) along with the appropriate organosiloxane modifier (0.5, 1.0, or 3.0 mmol), and the resultant mixture was heated at reflux temperature under nitrogen for 6 h. The reaction mixture was allowed to cool, and the silica was collected by filtration under air, washed with MeOH (3×25 mL) and acetone (2×25 mL), and then dried in vacuo (2 h) and then in an oven at 50 °C overnight. Samples for microanalysis were further dried in vacuo for 3 days. In addition to the data given below, IR spectra for all of the modified silicas are included in the Supporting Information.

General Method for the Immobilization of Palladium Nanoparticles on the Modified Silicas. To a degassed sample of the organically modified silica (1.00 g) under nitrogen were added toluene (60 mL) and palladium acetate (0.380 g, 1.69 mmol), and the resultant mixture was heated at 100 °C for 5 h. The silica was then collected by filtration under air, washed with MeOH (3×25 mL) and acetone (2×25 mL), and then dried in vacuo (2 h) and then in an oven at 50 °C overnight. Samples for microanalysis were further dried in vacuo for 3 days.

Materials Characterization. All solids were studied using nitrogen sorption to measure BET surface areas, total (Gurvitsch) pore volumes, and to characterize pore-size distributions (BJH method); the theoretical aspects of these analyses may be found in a number of standard texts on adsorption.²⁴ Nitrogen isotherms were measured at 77 K using an automated sorption equipment, the Micromeritics Tristar 3000. Data were collected on a PC, and calculations of surface and pore properties were subsequently performed using the Micromeritics software, TriStar 3000 v2.00. All samples were purged with flowing nitrogen gas at 150 °C for 3 h prior to analysis. Free space in the sample tube was determined with He, assumed not to adsorb, for each sample. FT-IR spectra were recorded for samples after being pressed into 13 mm disks with freshly dried KBr salt. Spectra were recorded at room temperature with a Nicolet 550 Magna IR spectrometer at a resolution of 4 cm⁻¹, with 32 scans per sample. Elemental analysis, for carbon, hydrogen, and nitrogen (CHN), was performed using a Carlo Erba 1110 CHN Elemental Analyzer. Analysis for palladium was performed using ICP-MS at the Johnson Matthey Technology Centre, Sonning Common, UK, and also atomic absorption spectroscopy using a Perkin-Elmer AAnalyst 100 spectrometer. Thermogravimetric analysis was performed using a Stanton Redcroft TG750 thermal analyzer, with a ~10 mg sample of each solid heated to 900 °C in air. Transmission electron microscopy was performed using a JEOL 1200EX instrument fitted with an Oxford Instruments ISIS 300 energy-dispersive X-ray analysis system. Solid samples were sonicated for few minutes in acetone, and a drop of the resultant suspension was applied to a carbon-covered 3 mm copper grid. Digital TEM images were recorded using a SIS Megaview II digital camera and analySIS 3.0 software.

General Method for the Suzuki Coupling of Aryl Bromides. The reaction was performed in a modified 100 mL three-necked flask, in which one of the necks was fitted with a sintered frit. A mixture of the appropriate aryl bromide (10.0 mmol), PhB(OH)₂ (1.83 g, 15.0 mmol), K₃PO₄ (4.24 g, 20.0 mmol), the appropriate silica supported palladium catalyst (60 mg), and hexadecane (internal standard, 0.10 mL) in toluene (30 mL) was heated at 110 °C under nitrogen for 5 h. After this time, an aliquot of the supernatant liquid (0.2 mL) was removed, added to HCl (2 M, 0.5

mL), extracted with toluene (3×1 mL), the combined organic extracts were dried (MgSO₄), and then the conversion was determined by GC analysis.

Time-Dependent Studies on the Coupling of Phenylboronic Acid with 4-Bromoanisole. These were performed as described above either at 110 or at 25 °C, and aliquots of the supernatant liquid (0.2 mL) were removed at various stages throughout the reaction for analysis by GC.

Recyclability Studies. The catalysis was performed as described in the general method except that after the sample had been removed for GC analysis the rest of the supernatant was removed via the fritted sinter. The residue was washed with toluene (2×30 mL), diethyl ether (30 mL), water (2×30 mL), diethyl ether (30 mL), and then dried in vacuo (8 h). After this time, the flask was recharged with substrates, base, and solvent and the reaction was repeated.

Results and Discussion

Synthesis and Characterization of the Palladium Catalysts. In recent work, one of us has showed that it is possible to use nanoparticulate palladium stabilized by tetrabutylammonium bromide (TBAB), in the presence of water, to couple deactivated (electron-rich) aryl bromide and chloride substrates,²⁵ and a prime aim of the current work was to test whether the TBAB-based catalyst or related systems could be successfully immobilized, and whether this immobilization would lead to recyclability. We thus prepared a range of organosiloxane-modified silicas, containing various amine functionalities ranging from primary to quaternary nitrogen centers. These are listed in Table 1. The silica chosen as support was commercially available Kieselgel 100, which has a nominal mean pore size of 100 Å. Surface area analysis (nitrogen sorption) of the batch used showed the mean pore size typically to be 120 Å by the BJH pore-size distribution curve and the surface area to be 275 m² g⁻¹. Table 1 contains the results of analysis studies for the organically modified silicas. The CHN analysis data confirm that the organic functionalization takes place with the intended ligands (analysis of the pure Kieselgel silica prior to modification showed only negligible amounts of carbon and nitrogen), and IR spectra showed for each organically modified material the presence of characteristic vibrational modes of the intended modifier (Supporting Information). The elemental analysis data in Table 1 show that for the materials **A**, **B**, and **C**, saturation with organic material is achieved at 1 mmol g⁻¹: further nominal loading results at best in only small increases in CHN content. This proves that excess organic material is completely washed from the sample and that the only organic species present is that covalently attached to the silica. For the materials **D–H**, we therefore always used an excess of organic modifier (nominally 3 mmol g⁻¹). Upon functionalization of the silica, the total surface area of the samples is observed to drop from the initial value of 275 m² g⁻¹, but all maintain a value of around 200 m² g⁻¹. Similarly, the mean pore diameter and total pore volume are seen to decrease for each of the modified samples, although not by significant amounts (see Table 1). Figure 1 shows typical

(24) See, for example: (a) Gregg, S. J.; Sing, K. S. W. *Adsorption, Surface Area and Porosity*, 2nd ed.; Academic Press: London, 1982. (b) Rouquerol, F.; Rouquerol, J.; Sing, K. S. W. *Adsorption by Powders and Porous Solids*; Academic Press: London, 1999.

(25) Bedford, R. B.; Blake, M. E.; Butts, C. P.; Holder, D. *Chem. Commun.* **2003**, 466.

Table 1. Characterization Data for the Organically Modified Silica Samples


modified silica R (see Scheme 1)	sample identifier	nominal loading of organic modifier (mmol/g)	analysis C, H, N, %	surface area, m ² /g	total pore volume, cm ³ /g	mean pore diameter, Å
[NBu ₃] ⁺	A0.5	0.5	6.98, 1.85, 0.50	235	0.73	86
	A1	1.0	8.33, 1.99, 0.61	222	0.67	82
	A3	3.0	7.80, 1.93, 0.56	225	0.69	84
	B0.5	0.5	3.26, 0.83, 0.89	232	0.79	94
	B1	1.0	5.22, 1.09, 1.58	207	0.68	88
	B3	3.0	5.54, 1.12, 1.72	204	0.66	88
NH ₂	C0.5	0.5	2.99, 1.14, 0.96	240	0.83	94
	C1	1.0	3.73, 1.17, 1.18	235	0.80	91
	C3	3.0	3.95, 1.27, 1.31	230	0.78	91
NHMe	D3	3.0	4.50, 1.08, 1.21	200	0.79	90
NEt ₂	E3	3.0	6.09, 1.39, 0.98	238	0.78	87
NHPh	F3	3.0	6.05, 0.88, 0.65	250	0.78	88
NHCH ₂ CH ₂ NH ₂	G3	3.0	6.17, 1.54, 2.70	203	0.70	88
NH(CH ₂) ₂ NH(CH ₂) ₂ NH ₂	H3	3.0	7.82, 2.06, 3.66	190	0.65	86

Table 2. Characterization Data for the Palladium-Loaded Organosilica Samples

modified silica	nominal loading of palladium/mg g ⁻¹	catalyst identifier	palladium analysis/mg g ⁻¹	analysis C, H, N, %	surface area, m ² /g	total pore volume, cm ³ /g	mean pore diameter, Å
A0.5	182	A0.5Pd	179	7.99, 1.91, 0.48	193	0.56	84
A1	182	A1Pd	175	8.54, 2.10, 0.56	189	0.53	79
A3	182	A3Pd	164	8.41, 2.04, 0.54	188	0.54	81
B0.5	182	B0.5Pd	169	6.57, 1.17, 0.86	220	0.61	84
B1	182	B1Pd	145	8.02, 1.45, 1.54	219	0.53	74
B3	182	B3Pd	178	8.54, 1.52, 1.38	208	0.52	77
C0.5	182	C0.5Pd	186	5.59, 1.08, 0.78	220	0.61	86
C1	182	C1Pd	158	5.95, 1.39, 1.04	220	0.60	81
C3	182	C3Pd	160	6.17, 1.34, 1.16	212	0.57	80
D3	182	D3Pd	179	5.56, 1.33, 1.08	214	0.60	82
E3	182	E3Pd	183	5.04, 1.33, 0.77	222	0.63	83
F3	182	F3Pd	172	5.67, 1.01, 0.54	240	0.65	84
G3	182	G3Pd	172	7.94, 1.76, 2.30	180	0.51	78
H3	182	H3Pd	169	9.03, 2.09, 2.90	170	0.46	75

nitrogen sorption isotherms recorded along with the results of BJH pore-size analysis. The sorption curves all may be described as Type IV according to the IUPAC definitions of porosity.²⁶ Type IV isotherms are characteristic of a mesoporous pore system, and the hysteresis loop observed arises from capillary condensation within the mesopores. We may conclude from the data in Figure 1 that upon organic modification the silicas maintain their mesoporosity and high surface area, with only a small reduction in total pore volume.

Table 2 shows characterization data for the palladium-loaded samples. The close agreement between the nominal Pd loading and that determined by AAS analysis shows that we have successfully loaded virtually all of the intended palladium onto the solid support. As with the organic modification, we observe a small drop in surface area, total pore volume, and mean pore diameter upon introduction of the palladium, but the porosity and total surface area are still high. The small reduction in surface area, pore volume, and pore diameter is totally consistent with the presence of immobilized species. CHN analysis of the Pd-containing solids shows a larger mass % of organic species than prior to the introduction of the metal. At first, this seems puzzling because the palladium must contribute a large percentage mass of the solids, but we propose that the palladium particles are stabilized by a surface coating of acetate. The TGA shows no evidence for any bulk palladium acetate: palladium acetate itself shows a distinct and sharp mass loss of 63% at

300 °C, which was never seen in any of the palladium-containing silicas. Thus, we suggest some surface acetate is responsible for the larger organic component of the composite solids. Further support for this idea is provided by IR spectra of the palladium-loaded solids, which show characteristic asymmetric and symmetric —COO^- stretches of acetate groups that are not present in the organic-modified silicas. These IR modes are shifted from bulk palladium acetate, suggesting free acetate groups in the solid.

The nitrogen sorption isotherms of the Pd-loaded solids, Figure 2a shows a typical example, indicate that the overall mesoporosity is maintained after the introduction of palladium. After several catalytic runs, however, the porosity and surface areas of the materials are diminished, as shown in Figure 2b and c. For example, after six catalytic runs, catalyst **G3Pd** shows a mean pore size of 70 Å, total pore volume of 0.15 cm³ g⁻¹, and surface area of 60 m² g⁻¹. This will be discussed below when we consider catalyst deactivation. TEM images of selected catalysts are presented in Figure 3. These reveal the presence of nanoparticulate palladium (verified by measurement of the EDXA spectrum of selected areas of sample) in the solid host. The palladium particles have typical diameters of 3–6 nm, and these remain after several catalytic runs: there is no evidence for sintering of the palladium particles. Powder X-ray diffraction (Supporting Information) verifies the presence of metallic palladium in the solids, and by analysis of the line broadening, an average particle size of 5 nm was determined, entirely consistent with the TEM results.

(26) Sing, K. S. W.; Everett, D. H.; Haul, R. A. W.; Moscou, L.; Pierotti, R. A.; Rouquerol, J.; Siemieniewska, T. *Pure Appl. Chem.* **1985**, *57*, 603.

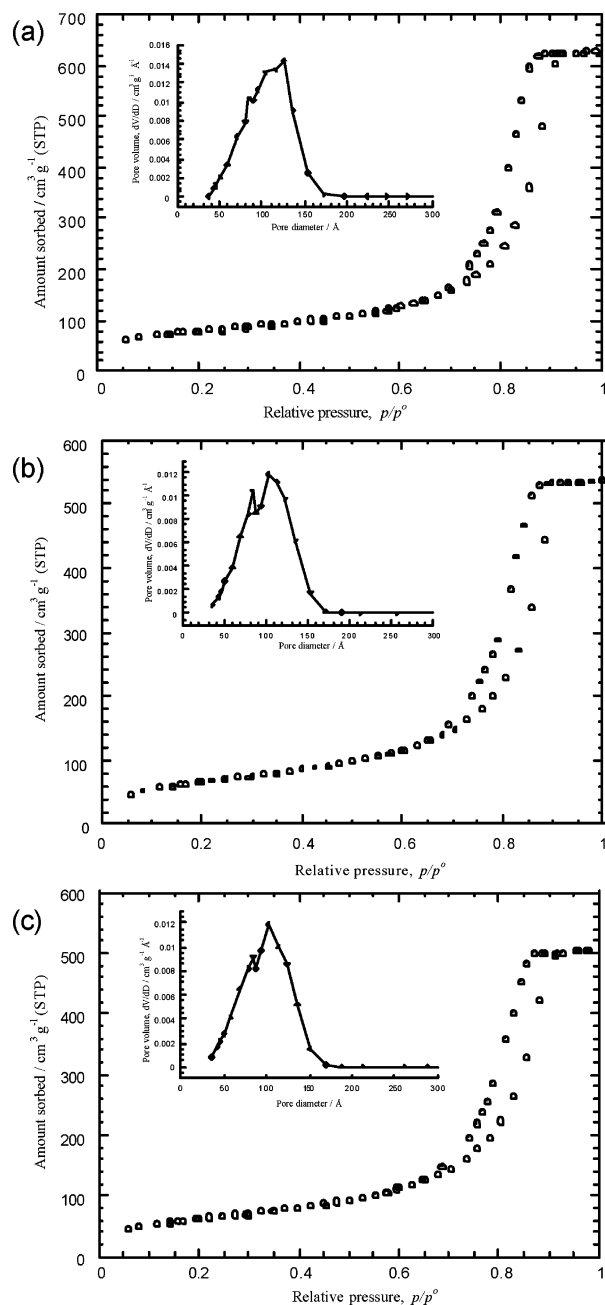


Figure 1. BET nitrogen sorption isotherms (77 K) for (a) the silica support prior to modification, (b) organic-modified support **C0.5**, and (c) organic-modified support **C3** (see Table 1). ○ represent sorption, and ● represent desorption. The inset is the BJH pore-size distribution curve.

Catalytic Testing. Scheme 2 shows the general coupling reaction we have focused upon in the current work.

Initially, a solvent/base optimization study was performed for the coupling of phenylboronic acid with 4-bromoanisole catalyzed by **C0.5Pd**, using toluene and 1,4-dioxane as solvents and K₂CO₃, K₃PO₄, Cs₂CO₃, KF, and KF:K₃PO₄ (1:1) as bases. 4-Bromoanisole was chosen as the test substrate because it is electronically deactivated with respect to oxidative addition and therefore gives a more accurate assessment of catalyst activity as compared to more easily coupled electron-deficient species, such as aryl iodides. The results of this study are presented graphically in Figure 4. This shows that optimum activity (assessed by measuring

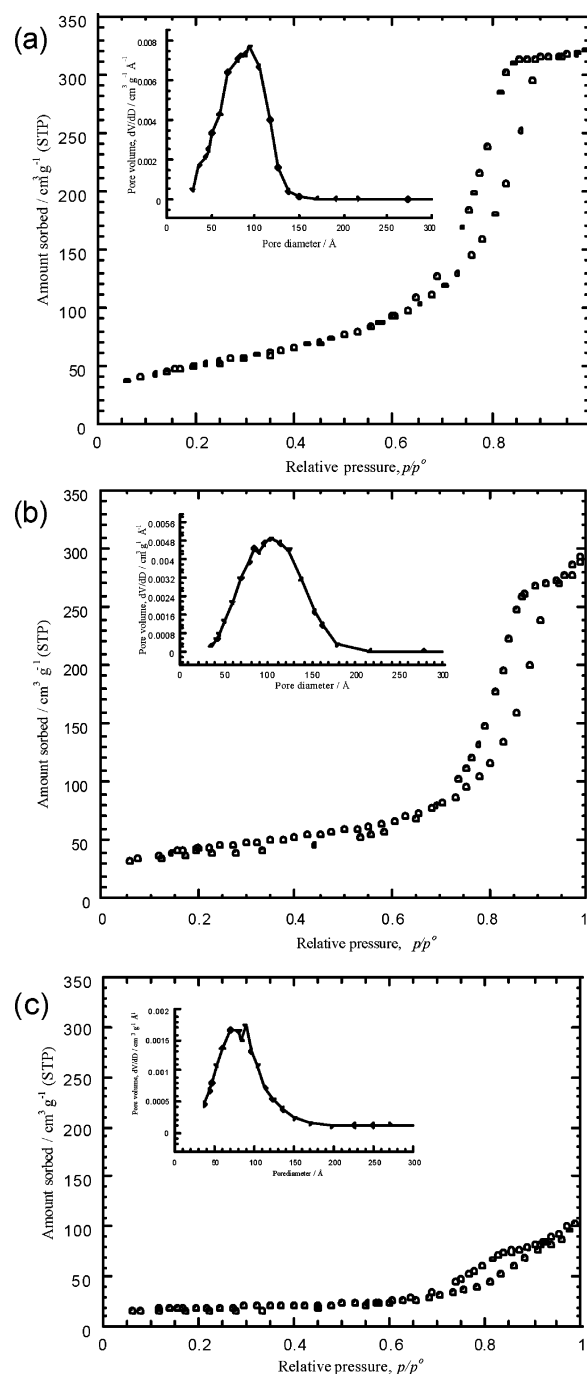
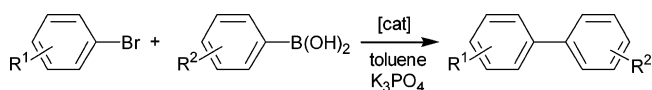


Figure 2. BET nitrogen sorption isotherms (77 K) for (a) catalyst **G3Pd** as-made, (b) catalyst **G3Pd** after three catalytic runs, and (c) catalyst **G3Pd** after six catalytic runs (see Table 2). ○ represent sorption, and ● represent desorption. The inset is the BJH pore-size distribution curve.

Scheme 2. Suzuki Coupling of Aryl Bromides



percentage conversion in 5 h) was obtained in toluene with K₃PO₄ acting as base, and these conditions were thus used for all further studies (it should be noted that the solvent-base optimization was repeated for the most active catalysts produced and K₃PO₄/toluene was found always to be the optimal combination). Temporal studies, performed using catalyst **C0.5Pd**, in the coupling of phenylboronic acid with 4-bromoanisole reveal that the maximum conversion is

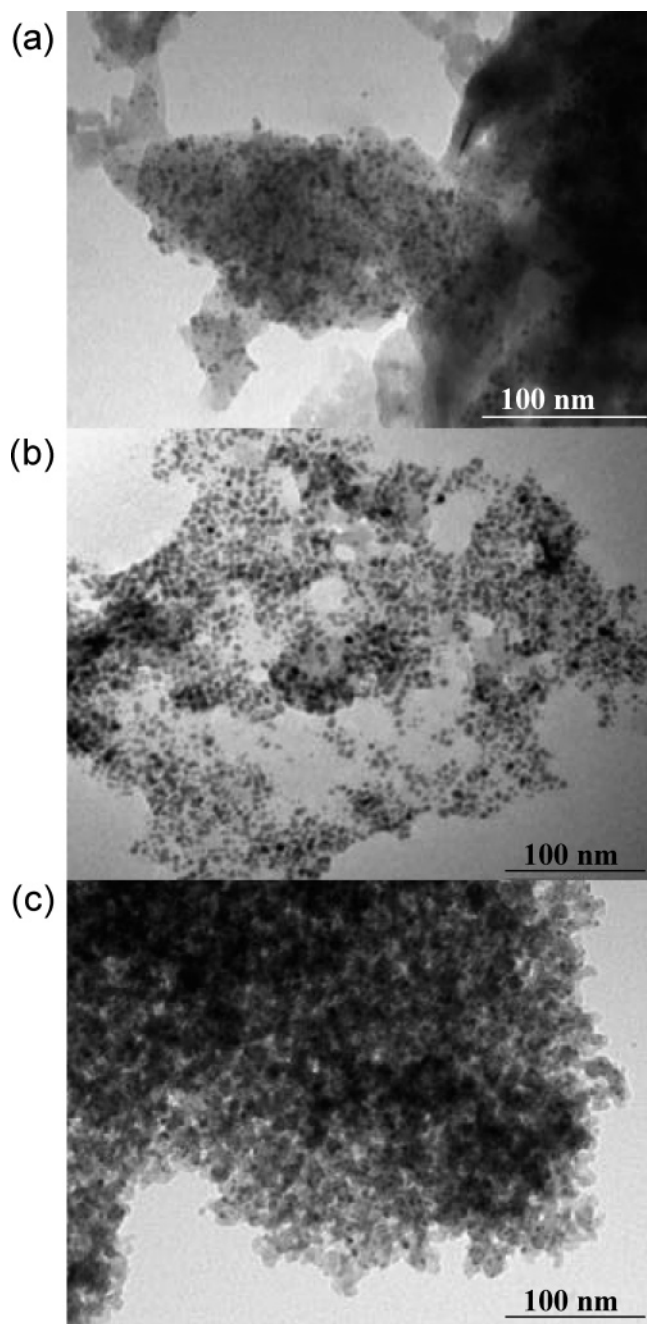


Figure 3. TEM images of (a) catalyst **G3Pd** as-made, (b) catalyst **G3Pd** after three catalytic runs, and (c) catalyst **G3Pd** after six catalytic runs.

achieved in ~ 1 h, even if activity decreases after repeated runs, Figure 5.

During detailed catalytic testing, we focused upon those materials with the highest organic component (nominally 3 mmol g⁻¹) because we had shown above that these materials suffer no significant reduction in surface area as compared to the materials with lower levels of organic functionalization. Table 3 shows the results of the catalysis survey. Initially, we focused upon the coupling of phenylboronic acid with 4-bromoanisole (entries 1–8 in Table 3). Catalyst **A3Pd** shows fairly poor activity in the coupling of phenylboronic acid with 4-bromoanisole (entry 1) despite the fact that the immobilized ammonium salt is very similar in structure to TBAB, which we have shown previously to stabilize active catalysts for this reaction in a homogeneous system.²⁵ We

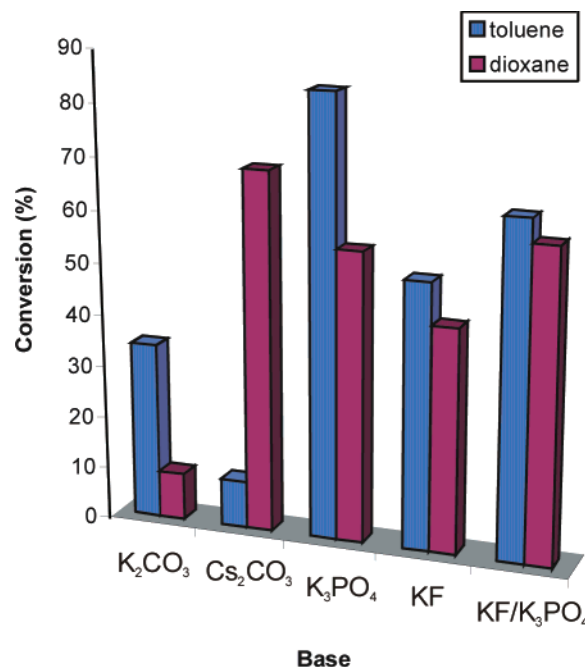


Figure 4. Bar chart showing catalyst activity in the solvent-base optimization for catalyst **C0.5Pd** (coupling of phenylboronic acid with 4-bromoanisole in K₃PO₄/toluene at 100 °C).

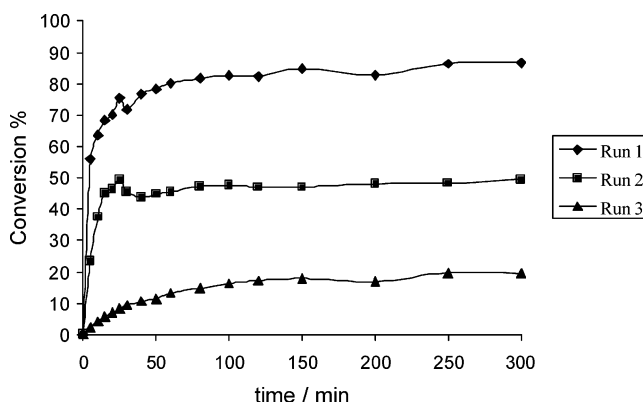


Figure 5. Temporal plot of catalytic activity for catalyst **C0.5Pd** over three recycles (coupling of phenylboronic acid with 4-bromoanisole in K₃PO₄/toluene at 100 °C).

Table 3. Use of Catalysts **3APd**–**3GPd** in the Suzuki Coupling of Aryl Bromides (See Scheme 2 for Labeling of R¹ and R²)^a

entry	R ¹	R ²	catalyst	conv. (%) ^b [run]
1	4-OMe	H	A3Pd	11[1], 21[2], 17[3]
2	4-OMe	H	B3Pd	40[1], 38[2], 39[3]
3	4-OMe	H	C3Pd	75[1], 76[2], 50[3]
4	4-OMe	H	D3Pd	82[1], 89[2], 37[3]
5	4-OMe	H	E3Pd	80[1], 64[2], 34[3]
6	4-OMe	H	F3Pd	33[1], 30[2], 15[3]
7	4-OMe	H	G3Pd	94[1], 95[2], 93[3]
8	4-OMe	H	H3Pd	98[1], 93[2], 90[3]
9	4-Me	H	G3Pd	90 [1]
10	4-COMe	H	G3Pd	95 [1]
11	2-Me	H	G3Pd	78 [1]
12	2-OMe	H	G3Pd	85 [1]
13	H	4-Me	G3Pd	76 [1]

^a All reactions were performed in K₃PO₄/toluene at 110 °C. ^b Conversion to Suzuki product monitored by GC with a hexadecane standard.

found that addition of varying amounts of water to the reaction does not lead to increased conversion to product, again in contrast with previous studies using TBAB.²⁵ The *N*-methyl-imidazolium-containing system **B3Pd** shows im-

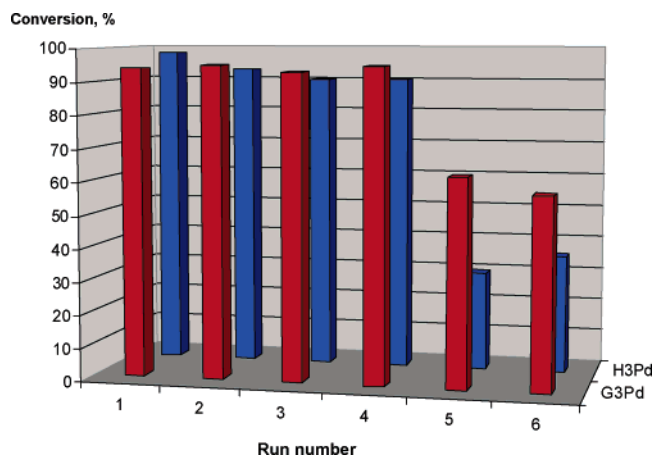


Figure 6. Bar chart showing catalyst activity for **G3Pd** over several recycles (coupling of phenylboronic acid with 4-bromoanisole in K_3PO_4 /toluene at 100 °C).

proved activity and good recyclability (entry 2); however, much better activity is observed when the ammonium salt headgroups are replaced by neutral amines. In general, primary and secondary alkylamines fare better than secondary alkylarylamines. While the tertiary alkylamine-containing system **E3Pd** shows good activity (entry 5), its recyclability is poorer than with primary and secondary alkylamine-containing systems (for example, compare with entries 3 and 4). Catalysts **G3Pd** and **H3Pd** gave the most promising results, in terms of activity and, more importantly, recyclability. TEM analysis of a sample of catalyst **G3Pd** taken after three catalytic runs shows that the nanoparticulate morphology of the catalyst remains, Figure 3, with essentially no evidence of sintering observed. Palladium analysis of solutions of crude product mixtures shows only low levels of palladium contamination, implying that catalyst leaching is not a problem over three runs. We therefore tested these materials over a larger number of runs, as summarized in Figure 6. As can be seen, both catalysts start losing activity after the fourth run, a trend that is particularly pronounced with **H3Pd**. While TEM analysis of **G3Pd** indicates that nanoparticulate palladium remains after six runs, AAS of both of the used catalysts after six runs shows that palladium leaching has now occurred (residual Pd loadings: **G3Pd**, 106 mg g⁻¹ and **H3Pd**, 78 mg g⁻¹). It seems that, while the catalysts are stable for a number of runs with low levels of leaching, they are prone eventually to a drop in activity. This has implications for catalysis testing in this type of system: the observation of a small number of runs with quantitative conversion is not an indication of genuine recyclability.

As a final test of the activity of catalyst **G3Pd**, which had shown the highest activity and recyclability, it was tested with a number of different substrates, as shown in Table 3. Catalyst **G3Pd** can be used to good effect with a number of different aryl bromides (entries 9–13, Table 3). Entries 8 and 9 show that similar activities are seen with more easily coupled aryl bromides, as might be expected. The introduction of steric bulk in the 2-position of the aryl bromide leads to a slight lowering of catalyst performance (entries 11 and

12), again, as would be anticipated. The result obtained in the coupling of bromobenzene with 4-tolyl-boronic acid (entry 13) is perhaps a little surprising because the ease of coupling of the bromide should lie between those of 4-bromotoluene and 4-bromoacetophenone (entries 9 and 10). Further, the higher nucleophilicity of the boronic acid should impart greater ease of coupling than with phenylboronic acid.

Finally, we compare our findings with other recent work that has utilized supported nanoparticulate palladium for Suzuki coupling reactions. We note that, in general, previous studies of catalysis of the Suzuki coupling reaction by nanoparticulate palladium catalysts have been performed using nonactivated, and hence less demanding, aryl iodides. Liu et al. used a polymer–palladium composite material but did not test their catalysts with deactivated aryl bromides but rather with nonactivated aryl iodides, and, in their case, activities dropped to ~80% after five recycles.²³ Narayanan and El-Sayed also studied polymer-supported palladium (in their case only for the coupling of the nonactivated iodobenzene and phenylboronic acid) and observed some sintering of the metal particles with a concurrent drop in activity.²¹ It would appear to be a general problem that all of the supported nanoparticulate Pd catalysts are prone to a drop in activity after prolonged recycling, although we do note that it is rare that materials have been previously tested beyond three or four runs to probe fully this phenomenon. In our case, we observe some palladium leaching after 4–6 runs, but we also observe both product and byproducts by IR spectroscopy in the used catalysts, suggesting that blocking of access to the active catalytic centers byproducts of the reaction is an additional cause of the drop in activity; this is further supported by the reduction in surface areas of the solids with repeated use.

Conclusions

The immobilization of palladium nanoparticles on amorphous, mesoporous silica, which has been modified by amine functionalities, provides a convenient means for the preparation of heterogeneous catalysts for the commercially important Suzuki-coupling reaction. The catalysts are very sensitive to the nature of the amine modification used, and by selecting diamine or triamine functionalities, we can prepare catalysts with high activity and a degree of recyclability. Further research into these and other related materials must focus upon maintaining activity over many catalytic runs: we have shown that even if initial high recyclability is observed for supported nanoparticulate palladium, deactivation of the catalyst can occur if it is used beyond three or four runs.

Acknowledgment. We thank the Open University for funding a Postdoctoral Research Fellowship for U.G.S., and Johnson Matthey plc for performing the ICP analysis.

Supporting Information Available: Table of principal IR bands and figure of powder XRD of **D3Pd** (PDF). This material is available free of charge via the Internet at <http://pubs.acs.org>.

CM048860S